EXPLOSION POINTS IN SKEW MAPS

by

Anne Stefanie Costolanski
A Thesis
Submitted to the
Graduate Faculty
of
George Mason University
in Partial Fulfillment of
The Requirements for the Degree
of
Master of Science
Mathematics

Committee:

_____   Dr. Evelyn Sander, Thesis Director

_____   Dr. Kathleen Alligood, Committee Member

_____   Dr. Timothy Sauer, Committee Member

_____   Dr. Klaus Fischer,
                                    Department Chairperson

_____   Dr. Peter Becker, Associate Dean
                                    for Graduate Studies, College of
                                    Science

_____   Dr. Vikas Chandhoke, Dean,
                                    College of Science

Date: _____   Summer Semester 2007
                                    George Mason University
                                    Fairfax, VA

Explosion Points in Skew Maps

A thesis submitted in partial fulfillment of the requirements for the degree of Master of Science at George Mason University

By

Anne Stefanie Costolanski
Bachelor of Science
Virginia Polytechnic and State University, 1988

Director: Dr. Evelyn Sander, Professor
Department of Mathematics

Summer Semester 2007
George Mason University
Fairfax, VA

Acknowledgments

I would like to thank my thesis advisor, Dr. Evelyn Sander, for her assistance, patience, and faith in my ability to do this work. Her encouragement throughout the past two years has been crucial in helping me complete this thesis and continue forward with my mathematics education.

I would also like to acknowledge the many friends that I have made over my lifetime, but in particular those who have helped me through the past seven years. You are more than just friends, you are my family, and I am eternally grateful for your unwavering support and unconditional love.

Table of Contents

List of Tables

List of Figures

Abstract

EXPLOSION POINTS IN SKEW MAPS

Anne Stefanie Costolanski, MS

George Mason University, 2007

Thesis Director: Dr. Evelyn Sander

This paper describes various chaotic behavior present in skew maps. Some aspects common in the study of dynamical systems are explored: the existence of homoclinic orbits, the behavior of manifolds, chaotic attractors, and period doubling cascades; and for each, the similarities and differences between the behavior for one-dimensional maps, two-dimensional diffeomorphisms, and skew maps are given.

While it is known that chaotic attractors and period doubling cascades are present in one-dimensional maps and two-dimensional diffeomorphisms as well as in skew maps, the existence of bifurcations that result in drastic changes in a chaotic attractor, namely crises and explosions, has not yet been shown for skew maps. Numerical examples are provided to demonstrate their existence, with comparisons to two-dimensional diffeomorphisms that exhibit similar behavior.

Chapter 1: Introduction

1.1 Dynamical Systems

At its most general, the definition of a dynamical system is a set of possible states together with a rule that determines the present state in terms of past states. Dynamical systems model a variety of behavior, from simple biological systems to more complex meteorological phenomenon, and as applications have spread into other scientific disciplines, the importance of studying and quantifying the behavior of dynamical systems has increased.

A mathematical definition of a discrete dynamical system is the process $X \mapsto F(X)$ where $F : R^n \rightarrow R^n$ acts on a variable $X \in S \subset R^n$. X represents the present state of the system, and F represents the rule that determines future values. Although dynamical systems can exist in any n-dimensional space, a great deal of information has been discovered on the behavior of one-dimensional systems, as well as two-dimensional systems for which F is a diffeomorphism. Thus, we will limit our analysis to these dimensions, and will detail the similarities and differences in the behavior of maps in these dimensions.

To determine how a particular state of a dynamical system evolves over time, it is necessary to know the asymptotic behavior of the system as a whole. It is also useful to know how changes in the system, or changes in the initial state, will affect future states. Our analysis of future states of a system begins by finding those whose

behavior is the easiest to predict.

1.2   Stability Analysis

One of the simplest rules associated with iterative maps is that which sends all initial states to one particular state over time. Thus, there exists one initial state that stays fixed for all time, and all nearby points converge to that state under iteration.

Mathematically, a point P $\in S$ such that $F(P) = $ P is called a fixed point [4]. P is considered to be a stable fixed point if for any $\epsilon > 0$ there is a $\delta > 0$ such that for all $X \in$ a δ-neighborhood of P, $|F^n(X) - P| < \epsilon$ for all $n \geq 0$ [7], and P is called an attracting fixed point (or a sink) if there exists an $\epsilon > 0$ such that for all $X \in$ an ϵ-neighborhood of P, $\lim_{k \to \infty} F^k(X) = P$ [4]. Similarly, the fixed point P could repel all iterates in a neighborhood of P: if there exists an $\epsilon > 0$ such that for all $X \in$ an ϵ-neighborhood of P, the iterates of X (other than P itself) eventually map outside of the neighborhood, then P is called a repelling fixed point or a source [4]. Determining the existence and stability of fixed points is a first step in describing the behavior of iterative maps.

To determine the stability of a fixed point P, we study a linear approximation of F and evaluate it at P to determine the behavior of points near P. In one dimension, the linear approximation is the derivative of F which is then evaluated at P: $F'(P)$. In two dimensions, it is the Jacobian $DF(P)$ of F evaluated at P:

$$DF(P) = \begin{bmatrix} \frac{d}{dx}f_1(P) & \frac{d}{dy}f_1(P) \\ \frac{d}{dx}f_2(P) & \frac{d}{dy}f_2(P) \end{bmatrix} \tag{1.1}$$

The resulting eigenvalues determine the stability of P. In the one-dimensional case,

the following theorem establishes the rules for stability of a fixed point:

Theorem 1.1 (Stability of Fixed Points [4]).

Let F be a map on R, and assume that P is a fixed point of F.

1. If $|F'(P)| < 1$, then P is a stable fixed point (sink).

2. If $|F'(P)| > 1$, then P is an unstable fixed point (source).

Note: For $|F'(P)| = 1$, stability is not determined by this theorem.

In the two-dimensional case, the eigenvalues of $DF(P)$ indicate the stability of P.

Theorem 1.2 (Stability of Fixed Points in two dimensions [4]).

Assume $F : R^2 \to R^2$, and P is a fixed point of F.

1. If the absolute value of each eigenvalue of $DF(P)$ is greater than 1, then P is a source.

2. If the absolute value of each eigenvalue of $DF(P)$ is less than 1, then P is a sink.

There is a special class of fixed points that are important in the study of dynamical systems. Saddle points are those fixed points P for which one eigenvalue of $DF(P)$, λ_-, has absolute value less than 1, and the other eigenvalue, λ_+, has absolute value greater than 1. For a saddle fixed point, there exists points in an ϵ-neighborhood of P, $N_\epsilon(P)$, whose iterates converge to P, and there are also points in $N_\epsilon(P)$ whose iterates leave the neighborhood after a certain period of time and never return to $N_\epsilon(P)$. Two sets of points are especially important in the study of fixed points: the set of points that converges to P upon forward iteration, called the stable manifold, and the set of points that converges to P upon backward iteration, or the unstable manifold. The mathematical definitions are:

Let F be a map on R^2, and let P be a saddle fixed or periodic point for F.

- The stable manifold of P is the set of points $\{X\} \subset S$ such that $|F^n(X) - P| \to 0$ as n $\to \infty$ [4].

- A point X_0 is in the unstable manifold of P if there exists a backwards orbit $\{...X_{-n}, ..., X_{-2}, X_{-1}, X_0\}$ of F where $F(X_{-n}) = X_{-n+1}$ with the property that $|X_{-n} - P| \to 0$ as $n \to \infty$.

To find the stable and unstable manifolds of P, we can use the linear approximation of F at P to determine the initial directions of the stable and unstable manifolds at P. The following theorem states this more precisely:

Theorem 1.3 (Stable Manifold Theorem [4]).

Assume F is continuously differentiable at the point P, and that F has a saddle fixed point P such that $DF(P)$ has one eigenvalue λ_- with $|\lambda_-| < 1$ and one eigenvalue λ_+ with $|\lambda_+| > 1$. Let V^+ be an eigenvector corresponding to λ_+, and V^- be an eigenvector corresponding to λ_-.

Then there exists a neighborhood of P such that both the local stable manifold S and local unstable manifold U of F (local means the portion of the manifold remaining in a small neighborhood of the fixed point. See [11]) at P are one-dimensional curves as smooth as F that contain P, and V^+ is tangent to U at P and V^- is tangent to S at P .

Thus in a small neighborhood around the point P, the eigenvalues and eigenvectors of $DF(P)$ provide valuable information for determining the local stable and unstable manifolds, which can be used to find the global stable and unstable manifolds of F at P.

1.3   Chaotic Behavior

We are also interested in the behavior of iterates of points not on the stable or unstable manifold of a fixed point P.

For a random point $X \in S$, we can define a forward limit set, or ω-limit set, as the set of all points $X_i \in S$ to which X converges under forward iteration. More formally, a point Y is an ω-limit point of X for F provided there exists a sequence n_k going to infinity as k goes to infinity such that $\lim_{k \to \infty} |f^{n_k}(X) - Y| = 0$ [11]. The set of all ω-limit points of X is the ω-limit set of X, denoted $\omega(X)$.

Similarly, for an invertible map, a point Y is an α-limit point of X for F provided there exists a sequence n_k going to minus infinity as k goes to infinity such that $\lim_{k \to \infty} |F^{n_k}(X) - Y| = 0$ [11]. If F is not invertible, then if there exists a backwards orbit $\{ \ ... \ X_{-n}, ..., X_{-2}, X_{-1}, X_0\}$ with $X_0 = X$ and a subsequence n_k going to minus infinity as k goes to infinity such that $|X_{n_k} - Y| \to 0$ as $k \to \infty$, then Y is an α-limit point of X. The set of all α-limit points of X is the α-limit set of X, denoted $\alpha(X)$.

For a saddle fixed point P, if there is an intersection between the stable and unstable manifolds of P, the point of intersection H is called a homoclinic point. In this case, a homoclinic orbit exists, which is an orbit whose α- and ω-limit sets are both the same fixed point [7]. It is also possible for the unstable manifold to converge to the stable manifold without a point of intersection. Thus, any homoclinic orbit limits to the fixed point P under both forward and backward iteration (see Figure 1.1).

Intersections between the stable manifold of one saddle fixed point X_1 and the unstable manifold of a different saddle fixed point X_2 can also occur. These points
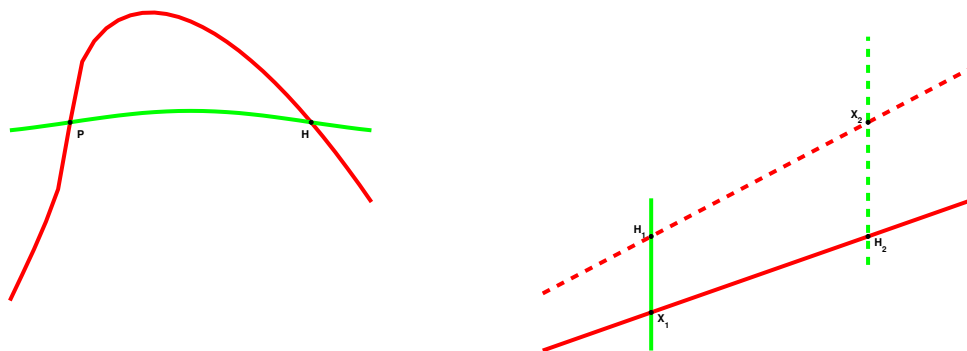
Figure 1.1: Homoclinic and heteroclinic orbits.

The graph on the left shows a homoclinic point H, with P as the fixed saddle point. The graph on the right has two heteroclinic points, with X_1 and X_2 as saddle fixed points and H_1 and H_2 as heteroclinic intersection points. For both pictures, the red lines are unstable manifolds and the green lines are stable manifolds.

are called heteroclinic points, and an orbit whose α-limit set is one fixed point and whose ω-limit set is another fixed point is called a heteroclinic orbit [7] (see Figure 1.1).

The ω-limit set can be a point, several points, or an infinite set of points. If the ω-limit set attracts a set of initial values with non-zero measure, it is called an attractor [4], and the set of initial values that limit to the attractor is called the basin of attraction.

The main focus of this paper is on chaotic behavior in two-dimensional maps. If F is a map in R^2, and $V = \{Y_1, Y_2,... \}$ is a bounded orbit of F, then the orbit is called chaotic [4] if:

1. V is not asymptotically periodic,

2. No Lyapunov number is exactly one, and

3. The largest Lyapunov number $L_1(Y_1) > 1$.

If $Y_1 \in V$ a chaotic orbit and $Y_1 \in \omega(Y_1)$, then $\omega(Y_1)$ is called a chaotic set, and a chaotic attractor is defined as a chaotic set that is also an attractor [4]. Chaotic attractors exist for both one-dimensional maps and two-dimensional diffeomorphisms.

Determining whether a particular map will generate a chaotic attractor is not obvious. For example, the map f(x) = 4x(1-x) generates a chaotic attractor as the ω-limit set of iterates of the unit square. However, a similar map, f(x) = 2x(1-x), generates a fixed point as the ω-limit set of the same set of initial values. There is very little difference between these two maps other than the factor multiplying x(1-x). So it cannot be assumed that maps that appear similar in structure exhibit the same limiting behavior.

1.4 One Parameter Families

In order to study the change in the behavior of a family of maps, such as the f(x) = x(1-x) example above, a parameter can be introduced into the map and allowed to vary continuously so that changes in the dynamics of the map can be identified. Significant changes in the behavior of a map take place at a bifurcation, which is defined as a change in the set of fixed or periodic points, or other sets of dynamic interest [4]. The value of the parameter at which the change takes place is called the bifurcation value. A map may have more than one bifurcation value for a set of initial conditions; in fact, in many cases, a map has infinitely many bifurcations.

An infinite sequence of bifurcation values in which the period of the attracting orbit doubles with each successive bifurcation is called a period-doubling cascade.

Period-doubling cascades are common in chaotic maps, and uniform properties that hold for cascades in both one-dimensional maps and two-dimensional diffeomorphisms have been discovered.

Chaotic attractors are also subject to bifurcations. A bifurcation of a chaotic attractor indicates either their appearance or disappearance, or a change in the structure of the attractor. A discontinuous change in the size of a chaotic attractor as a parameter is varied is called a crisis [3], and numerous examples exist in both one-dimensional maps and two-dimensional diffeomorphisms. In particular, the logistic map undergoes a crisis just past $\lambda \approx 3.82$, when the attractor changes suddenly from a chaotic orbit to a period three orbit.

A specific type of crisis is an explosion, which is a bifurcation in which new recurrent points form discontinuously far from any previously recurrent points [3]. To give a more precise definition of an explosion, we must define several concepts:

For an iterated function F, there is an ϵ-chain from X to Y when there is a finite sequence $\{Z_0, Z_1, ..., Z_N\}$ such that $Z_0 = X$, $Z_N = Y$, and $|F(Z_{n-1}) - Z_n| < \epsilon$ for $0 \leq n \leq N$ [3].

If there is an ϵ-chain from X to itself for every $\epsilon > 0$ (where $N > 0$), then X is said to be chain recurrent. The chain recurrent set is the set of all chain recurrent points. For a one-parameter family F_λ, we say (X, λ) is chain recurrent if X is chain recurrent for F_λ [3].

A chain explosion point (X, λ_0) is a point such that X is chain recurrent for F_{λ_0}, but there is a neighborhood N of X such that on one side of λ_0, no point in N is chain recurrent for F_λ [3].

Chain explosions (or explosions) can be caused by intersections between stable

and unstable manifolds, which cause a bifurcation from no homoclinic point to a homoclinic point. [1,3,13]. It is the purpose of this paper to show that specific bifurcation behaviors associated with chaotic attractors, specifically crises and explosions, are present in a particular type of two-dimensional map called a skew map, which is defined in the next chapter.

Chapter 2: Chaotic Behavior in Skew Maps

2.1 Skew Maps

Skew maps in R^2 are of the form $F(x,y) = (f(x), g(x,y))$ where x,y $\in R$. Although there are examples of piecewise continuous functions that lead to chaotic behavior in skew maps, we will limit most of our analysis to those maps with continuously differentiable functions f and g.

To determine the behavior of iterates near a fixed point, the linear approximation of the system can be used to evaluate the stability of a fixed point, although it may not always lead to a conclusive result. Since we are limiting our discussion to skew maps that are continuously differentiable, the behavior of the linearized system at a fixed point $P = (x_0, y_0)$ can be computed using the Jacobian matrix:

$$DF(x_0, y_0) = \left[\begin{array}{cc} f_x(x_0) & 0 \\ g_x(x_0, y_0) & g_y(x_0, y_0) \end{array} \right] \tag{2.1}$$

The eigenvalues of the system are $f_x(x_0)$ and $g_y(x_0, y_0)$, and have corresponding eigenvectors $\left(\begin{array}{c} \frac{f_x(x_0,y_0)-g_y(x_0,y_0)}{g_x(x_0,y_0)} \\ 1 \end{array} \right)$ and $\left(\begin{array}{c} 0 \\ 1 \end{array} \right)$. Since saddle fixed points produce some of the most interesting chaotic behavior, we assume that P is a saddle fixed point with either: (i) $|f_x(x_0)| > 1$ and $|g_y(x_0, y_0)| < 1$, or (ii) $|f_x(x_0)| < 1$ and $|g_y(x_0, y_0)| > 1$. By the Stable Manifold Theorem, for case (i), the linear subspace in the direction of

the eigenvector $\begin{pmatrix} 0 \\ 1 \end{pmatrix}$ is tangent to the stable manifold; for (ii), it is tangent to the unstable manifold. In either case, however, the linear subspace is equal to, rather than being merely tangent to, the stable or unstable manifold. This is due to the restriction that $x \mapsto f(x)$, and thus if an iterate of a point (x, y) maps to (x_0, y^*), where (x_0, y_0) is a fixed point, all forward iterates of (x_0, y^*) will remain on the line $x = x_0$. This restriction makes the stable or unstable manifold corresponding to the eigenvalue $|g_y(x_0, y_0)|$ very easy to compute.

The linear subspace in the direction of the other eigenvector, $\vec{V_1} = \begin{pmatrix} \frac{f_x(x_0,y_0)-g_y(x_0,y_0)}{g_x(x_0,y_0)} \\ 1 \end{pmatrix}$, is tangent to either the stable or unstable manifold (depending on the value of $|f_x(x_0)|$) at the fixed point P. As we shall see, unstable manifolds tangent to this direction can display some behavior different from that in two-dimensional diffeomorphisms.

2.2   Numerical Computation

To analyze the behavior of continuously differentiable skew maps, MATLAB and Dynamics software were used to plot the behavior of iterates and analyze the stability of fixed and periodic points.

For all graphs contained in this paper, MATLAB was used to generate the results. Since the Dynamics software is easier to use in finding the stability of fixed points, it was used to determine the stability of periodic points where needed.

Two main types of graphs were plotted:

- Stable and unstable manifolds of fixed points, and
- Chaotic attractors.

2.2.1 Stable and Unstable Manifolds

To plot the stable and unstable manifolds of a fixed point (x_0, y_0), the fixed point was determined analytically, as were the corresponding eigenvectors. These values were used as the initial data to generate the graph.

The manifold in the $\vec{V_0} = \begin{pmatrix} 0 \\ 1 \end{pmatrix}$ direction was plotted as a straight line. If the manifold consisted of only a portion of the $x = x_0$ line, the boundaries were computed analytically, and graphed accordingly.

For an unstable manifold tangent to the $\vec{V_1}$ direction, it was plotted by partitioning a small line segment of the linearized direction into K points, and iterating those points I times using the F map. The line segment used was between $\frac{1}{10}$ and $\frac{1}{1000}$ of the distance along the $\vec{V_1}$, depending on the amount of accuracy needed.

For a stable manifold in the $\vec{V_1}$ direction, the method used was similar to the above, where a line segment in the $\vec{V_1}$ direction was partitioned into K points and iterated I times. However, the function used to iterate the partition points was the inverse of F, which was calculated analytically.

2.2.2 Chaotic Attractors

In several cases, it was worthwhile to isolate the attractor by iteration of random points in the basin of attraction. Thus, a number K of random points were chosen and then iterated N times. The first I iterates of each point were dropped, and the next N-I iterates were plotted.

For the graphs involving a two piece attractor, the plot color was alternated between red and blue based on whether the iterate was an odd or an even number. This

allowed the two pieces of the attractor to show up distinctly on the graph.

For the graphs involving an attractor with an explosion point, the Nth iterate was plotted as a large blue dot to demonstrate whether the ω-limit set had changed at λ_0.

For all chaotic attractor graphs, part of the stable manifold of the fixed point X_0 that merges with the attractor was plotted. For both types of attractor graphs, due to the design of f(x), the stable manifold consists of multiple vertical lines $x = x_0$, $x = x_1$, $x = x_2$, ... , where (x_0, y_0) is the fixed point and x_1 and x_2 are preimages of either x_0 or another preimage of x_0. The preimages were calculated analytically.

2.2.3 Additional Information

Several other functions were plotted using MATLAB, and the method for calculation is explained as they appear in the text.

The Dynamics software was used to determine the existence and stability of several sets of periodic points near the attractor with an explosion point. It was also used to determine the stability of a set of periodic points that are the terminal values of the unstable manifold of the fixed point X_2 in the graph that demonstrates unstable manifolds crossing each other.

2.3 Homoclinic Orbits

Homoclinic orbits have been studied in one-dimensional maps and two-dimensional diffeomorphisms as well as in skew maps. In one dimension, a fixed or periodic point with a one-dimensional unstable manifold and a non-trivial zero-dimensional stable manifold that intersect is called a snap-back repeller [10]. The homoclinic orbit consists of the fixed point and the measure zero set. For diffeomorphisms, not only

do homoclinic and heteroclinic orbits exist, but tangencies between them are known to produce complex chaotic behavior [1–3].

There are constraints for skew maps to assure the existence of a homoclinic orbit. Since $x \mapsto f(x)$, a homoclinic orbit must exist in the x direction in order for an orbit to be homoclinic for the full skew map. Thus a homoclinic point of a skew map is a snap-back repeller in the x-direction. However, the addition of another dimension in skew maps over one-dimensional maps allows for multiple homoclinic orbits to exist for the same set of x-values.

While homoclinic orbits have been shown to exist in skew maps, most of the recent literature focuses on piecewise continuous functions that prove various conjectures regarding the lack of an infinite ω-limit set containing periodic orbits [5,6,9]. However, an example of a continuously differentiable function with a homoclinic orbit can be easily constructed using

$$f(x) = 4x(1-x), \quad g(x,y) = y(y+2)(1-x). \tag{2.2}$$

The point $(x_0, y_0) = (0,0)$ is a fixed point of equation (2.2), and a homoclinic orbit can be constructed by determining the preimages of x_0 and calculating the corresponding values of y. A sample homoclinic orbit is shown in Table 2.1.

Table 2.1: The first 13 iterates of a homoclinic orbit

Preimage	$\approx x$	$\approx y$
-	0	0
1	1.0	0.200536
2	0.5	0.183669
3	0.146447	0.102353
4	0.038060	0.051857
5	0.009607	0.025846
6	0.002408	0.012871
7	6.023×10^{-4}	0.006419
8	1.506×10^{-4}	0.003205
9	3.765×10^{-5}	0.001601
10	9.412×10^{-6}	0.000800
11	2.353×10^{-6}	0.000400
12	5.883×10^{-7}	0.000200
13	1.471×10^{-7}	0.000100

The orbit was calculated using MATLAB for the preimages of $x = 1$. The inverse function $f^{-1}(x) = \frac{1-\sqrt{1-b}}{2}$, where b is the value of the preimage, is used to compute the x-values of the homoclinic orbit. To compute the y values, a value for the 13th iterate is chosen close to $y_0 = 0$, and the values for y are iterated forward from the 13th down to the 1st preimage.

In this example, the values of y are not unique in forming a homoclinic orbit, since g(x,y) = xh(y) forces the orbit to be homoclinic in the y direction as soon as x = 0. The homoclinic orbit appears as Figure 2.1.
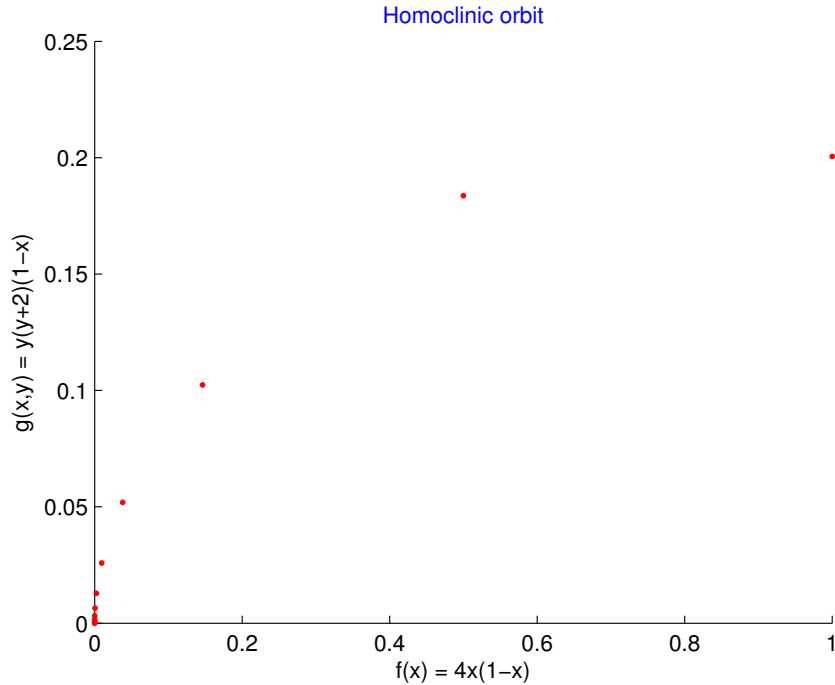
Figure 2.1: Skew map homoclinic orbit.

The red dots are the values of the first 13 iterates of a homoclinic orbit. The full homoclinic orbit is an infinite set of points.

Tangencies of homoclinic and heteroclinic orbits play a key role in determining whether crises and explosions exist in a particular map. In two-dimensional diffeomorphisms, the stable and unstable manifolds must be connected; however, this is not a requirement for other two-dimensional maps, as we shall see.

2.4 Behavior of Unstable Manifolds

This section describes the differences between the behavior of unstable manifolds for one-dimensional maps, two-dimensional diffeomorphisms, and skew maps.

It would seem obvious that the dynamics of stable and unstable manifolds in one

dimension would be trivial; however, that is not always the case. Snap-back repellers, which are responsible for homoclinic orbits in one-dimensional maps, have a one-dimensional unstable manifold and a non-trivial zero-dimensional stable manifold. However, reversing the dimensions of the manifolds such that the stable manifold is one-dimensional and the unstable manifold is zero-dimensional is not possible [3].

For two-dimensional diffeomorphisms, two unstable manifolds cannot cross each other since by definition the backward iterates of a fixed point must converge to the fixed point. If two unstable manifolds did cross, then there would exist an orbit along the unstable manifold of the first fixed point for which the backward iterates would converge to the other fixed point, which is contrary to the definition for unstable manifolds.

However, since skew maps are not always diffeomorphisms, they do allow two unstable manifolds to cross in certain cases.

Using the quadratic map

$$f(x) = 1 - \lambda x^2, \quad g(x, y) = 1 - Ay^2 - Bx^2 \tag{2.3}$$

with $\lambda = 0.65$, A $= 1$ and B $= 0.125$, four fixed points were found. The coordinates of the fixed points, corresponding eigenvalues, and stability are listed in Table 2.2:

Table 2.2: Fixed points of the quadratic map and their stability.

Fixed point	x_0	y_0	λ_1	λ_2	Stability
X_1	-2.2287	0.2932	2.8974	-0.5863	Saddle
X_2	0.6903	0.5911	-0.8974	-1.1821	Saddle
X_3	-2.2287	-1.2932	2.8974	2.5863	Source
X_4	0.6903	-1.5911	-0.8974	3.1821	Saddle

So X_3 is a repelling fixed point, and the other fixed points are saddles.

To analyze the behavior of the stable and unstable manifolds, the fixed points and their stable and unstable manifolds are graphed. For the source X_3, the strong unstable manifold is graphed, which is the curve that is locally tangent to the eigenvector associated with the larger eigenvalue of $DF(X_3)$. To graph the stable manifolds, the inverse of F is calculated:

$$f^{-1}(x) = \pm\sqrt{\frac{1-x}{\lambda}}, \quad g^{-1}(x,y) = \pm\sqrt{\frac{\lambda - \lambda y - B + Bx}{\lambda A}} \qquad (2.4)$$

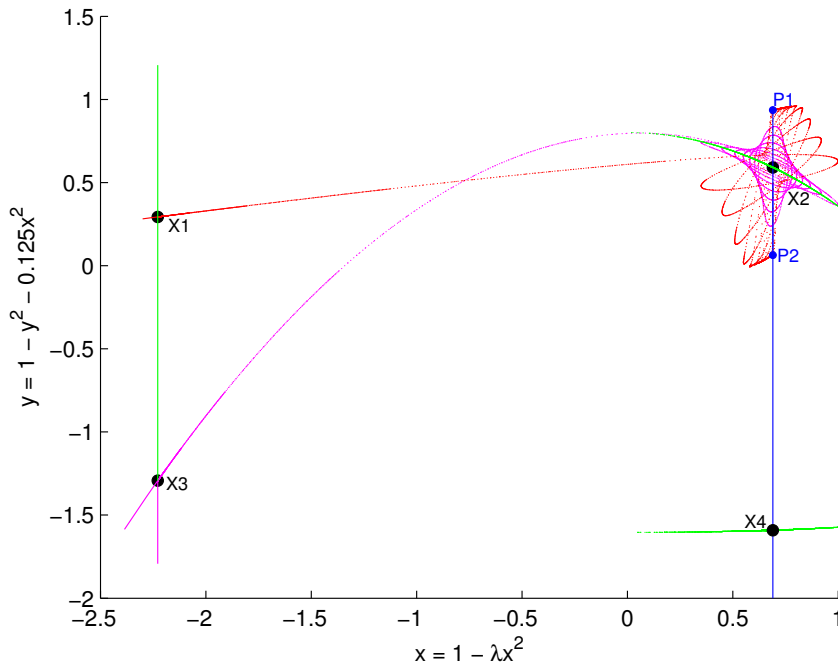The result is shown in Figure 2.2.

Figure 2.2: Stable and unstable manifolds for the quadratic system.

The stable manifolds are shown in green, and the unstable manifolds in red and blue for X_1 and X_2/X_4 respectively. The magenta line is the strong unstable manifold of X_3. Both branches of the unstable manifold of X_2 limit to a period two orbit, denoted P_1 and P_2. The upper branch of the unstable manifold of X_4 also limits to P_2.

It is clear that the restriction placed on unstable manifolds for two-dimensional diffeomorphisms is not applicable for skew maps. The unstable manifold of X_1 and the strong unstable manifold of X_3 cross each other multiple times as they approach the fixed point X_2. In addition, the unstable manifold of X_2 is also crossed multiple times as the unstable manifold of X_1 and the strong unstable manifold of X_3 limit to the attracting period two orbit.

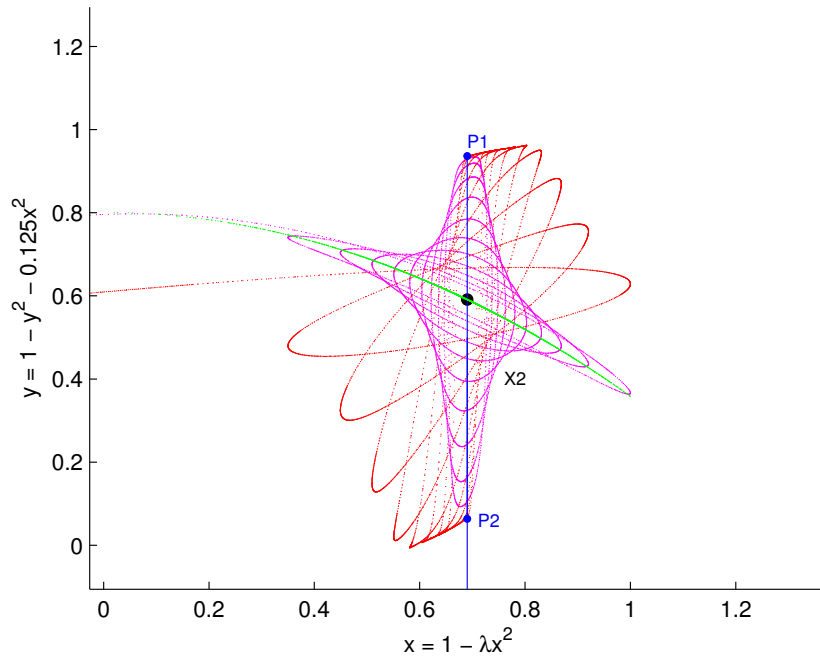A closer view of the fixed point X_2 shows this more clearly (see Figure 2.3).

Figure 2.3: A magnification of the behavior around the fixed point X_2.

The red line is the unstable manifold of X_1, and the magenta line is the strong unstable manifold of X_3. The unstable manifold of X_2 is shown in blue, and terminates at each point in the period two orbit. The remaining portion of the blue line below the period two orbit is the unstable manifold of X_4.

In addition to the unstable manifold crossings, the stable manifold of X_2 is crossed multiple times by both the unstable manifold of X_1 and the strong unstable manifold of X_3.

Thus the behavior allowed for stable and unstable manifolds is different for skew maps than for two-dimensional diffeomorphisms. The behavior of this skew map matches more closely with the behavior of manifolds in one dimension, in which a non-trivial zero dimension stable manifold can lie within a one-dimensional unstable manifold.

Period doubling behavior, however, is more standard for all three types of maps.

2.5   Period Doubling

Period doubling has been extensively studied for both one-dimensional maps and two-dimensional diffeomorphisms [4, 11]. The one-dimensional logistic map, $f(x) = \lambda x(1-x)$, is well known for the period doubling bifurcations that take place between $3 \leq \lambda < 4$. In two dimensions, there are many maps that produce period doubling bifurcations, including the Hénon map

$$f(x,y) = a - x^2 + by, \quad g(x,y) = x \tag{2.5}$$

In both one- and two-dimensional cases, a period doubling cascade drives the bifurcation values, with the difference between successive bifurcation values decreasing more rapidly as the parameter value increases. Feigenbaum calculated the rate of convergence of the bifurcation values by means of the limit $\delta = \lim_{n \to \infty} \frac{b_{n-1} - b_{n-2}}{b_n - b_{n-1}}$ where b_n is the nth bifurcation value. Feigenbaum discovered that the constant δ is the same for several different families of functions, and the value for those families, $\delta = 4.669202...$, is known as Feigenbaum's constant [11]. Several well-known maps, including the one-dimensional quadratic and logistic maps as well as the two-dimensional Hénon map, have Feigenbaum's constant as the limiting value of the bifurcation ratio.

For skew maps, the quadratic map listed in the previous section as system (2.3) has been shown to produce period doubling behavior for certain ranges of parameter values, and the limit of the ratio of the change in the bifurcation values has been shown to approach Feigenbaum's constant [12]. Thus we are interested in knowing whether period doubling can be found in other skew maps as well.

This is indeed true for

$$f(x) = \lambda x(1-x)^2(1+x), \quad g(x,y) = a - x^2 + by \tag{2.6}$$

with a $= 1.4$ and b $= 0.3$. The above system has a fixed point X_0 at (0,2) for any value of the parameter λ. As λ is increased beyond $\lambda = 1$, the number of fixed points that the left branch of the unstable manifold of X_0 converges to undergoes a period doubling cascade. The sequence of bifurcations begins when the fixed point appears for $\lambda > 1$ (see Figure 2.4).
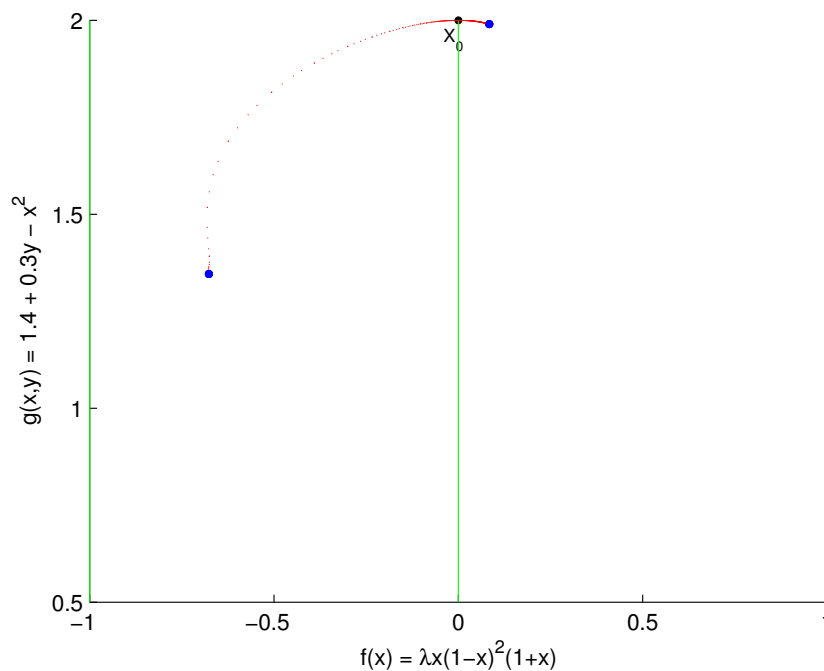

Figure 2.4: The stable and unstable manifolds of X_0 for $\lambda = 1.1$.

Both branches of the manifold, shown in red, converge to a fixed point on either side of the x = 0 portion of the stable manifold, shown in green. Other branches of the stable manifold, x = 1 and x = -1, are also shown in green.

As λ is increased past the first bifurcation value at approximately 1.25, the stability of the fixed point changes, and an attracting period two orbit is born (see Figure 2.5).
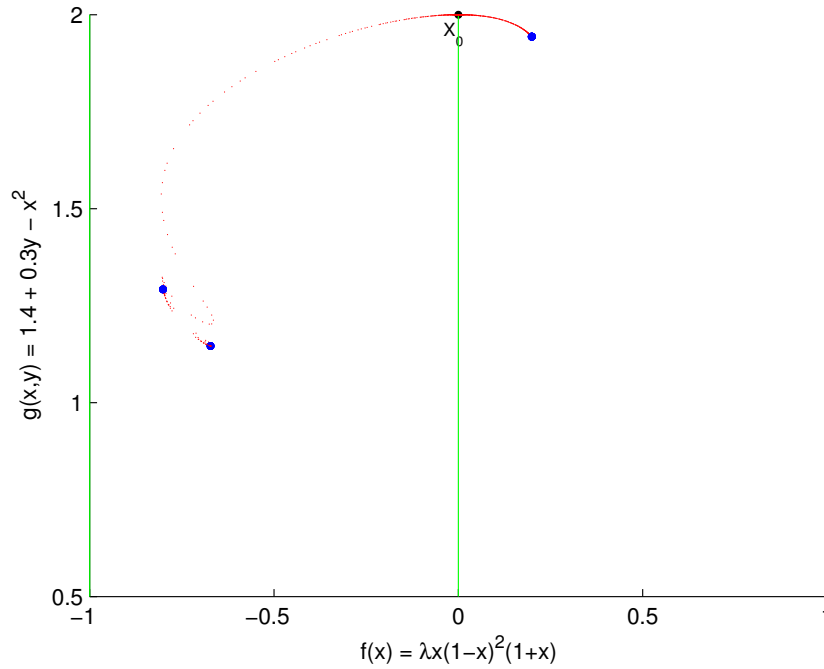

Figure 2.5: The stable and unstable manifolds of X_0 for $\lambda = 1.3$.

The left branch of the unstable manifold converges to a period two orbit.

As λ continues to increase, the bifurcation values appear more rapidly. The next bifurcation from a period two orbit to a period four orbit takes place at $\lambda \approx 1.38$ (see Figure 2.6).
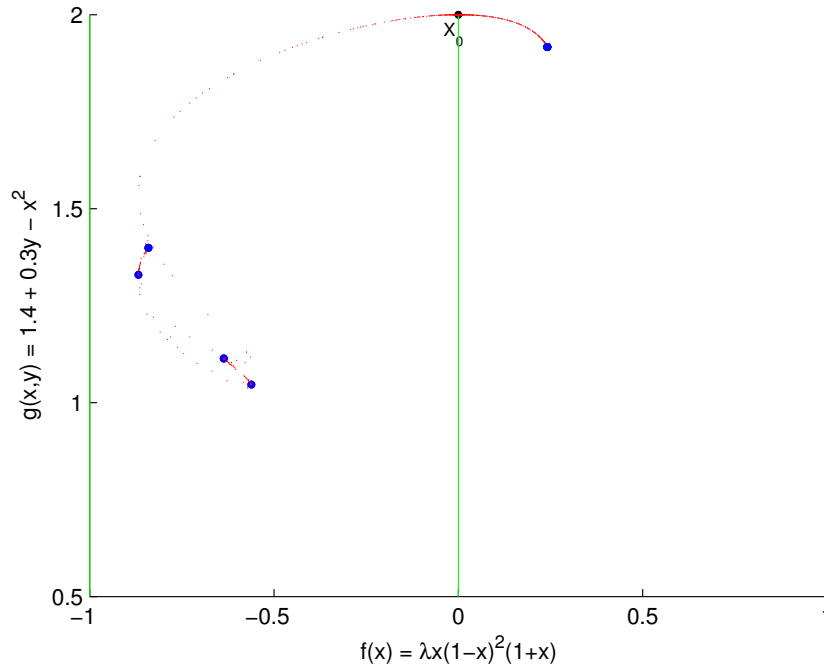

Figure 2.6: The stable and unstable manifolds of X_0 for $\lambda = 1.4$.

The left branch of the unstable manifold now converges to a period four orbit.

The period doubling cascade continues as λ is increased past the next bifurcation value at ≈ 1.41, with the onset of chaos at a value of λ around 1.43 (see Figure 2.7).
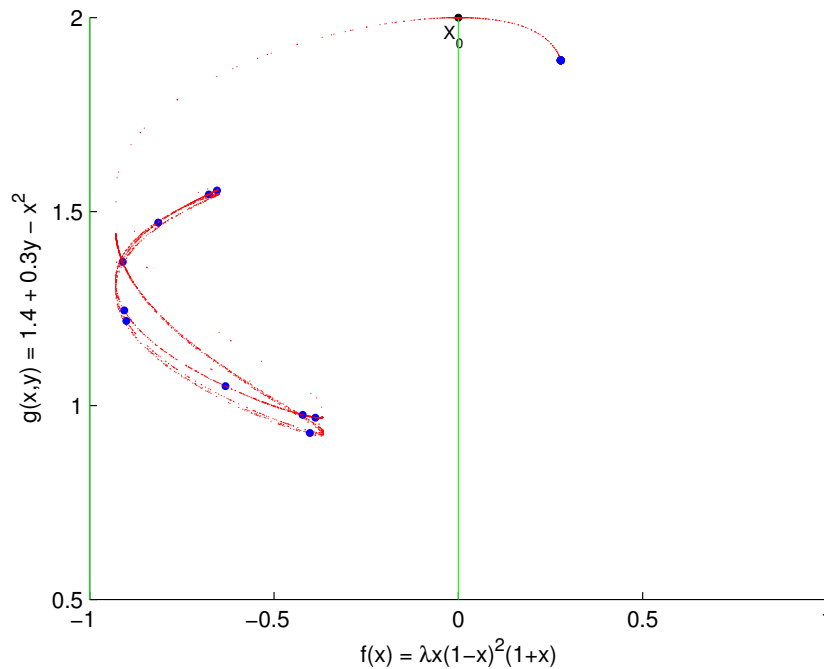

Figure 2.7: The stable and unstable manifolds of X_0 for $\lambda = 1.5$.

The left branch of the unstable manifold has become a chaotic attractor, while the right branch continues to converge to a fixed point.

The increasing rapidity of changes in bifurcation values support the idea that the skew map system shown as equation (2.6) satisfies Feigenbaum's law. Some sample data, shown in Table 2.3, also supports this view.

Table 2.3: Bifurcation values for the skew map, and the Feigenbaum ratio

Period	$b_n = \lambda$	ratio
2	1.247747	
4	1.380406	
8	1.412076	4.188791
16	1.419680	4.164913

32 points near the initial fixed point X_0 were iterated 4,000 times, and the values of the final iterates were analyzed. Starting at $\lambda = 1$, λ was increased until the number of distinct values of the 32 final iterates no longer matched the current period.

The ratios of the bifurcation values in this small data sample average ≈ 4.177 rather than the well-known constant associated with the Hénon map ≈ 4.669. However, due to the low number of periods calculated as well as possible loss of precision due to rounding, it is possible that the ratio limits to the same constant found for the Hénon map.

Thus the system (2.6) exhibits period doubling, which is consistent with the behavior for one-dimensional maps and two-dimensional diffeomorphisms.

2.6   Chaotic Attractors

Since period doubling cascades are present in skew maps, it is clear that skew maps can generate chaotic attractors. This has been shown for skew maps with quadratic f(x) and g(x,y) [12], and for a piecewise continuous f(x) with a quadratic g(x,y) [8]. For the map defined by equation (2.6), Figure 2.7 shows that an attractor exists for $\lambda = 1.5$, and for the quadratic map given by equation (2.3), setting $\lambda = 2$ changes the ω-limit set of points near the unstable manifold of fixed point X_1 and the strong unstable manifold of X_3 from an attracting period two orbit to a chaotic attractor
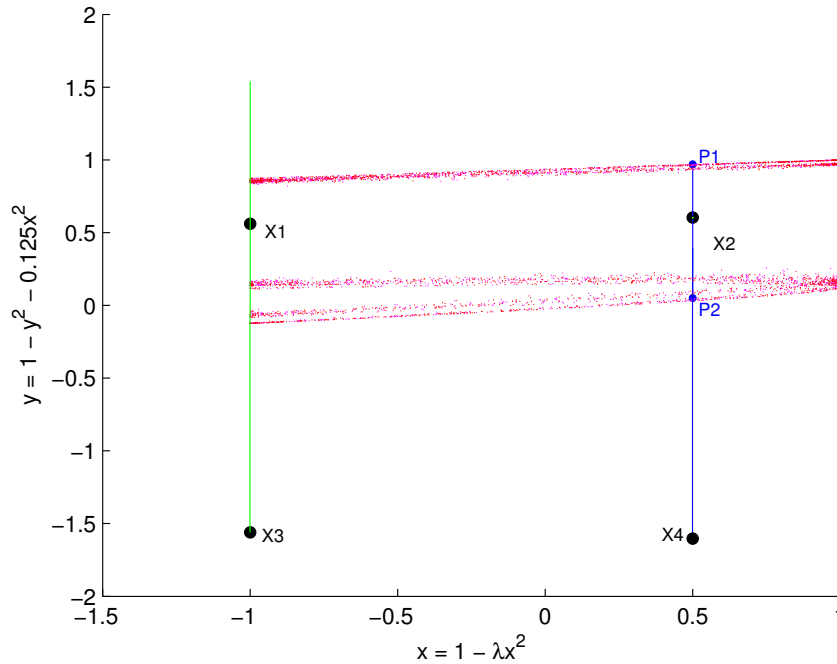
(see Figure 2.8).

Figure 2.8: The quadratic map at $\lambda = 2$.

The first 1,001 to 1,250 iterates of points on the unstable manifolds of fixed points X_1 and X_3 were plotted in red and magenta respectively. The iterates are bounded by the stable manifold of X_1, $x = -1$, on the left and by the line $x = 1$, the preimage of $x = -1$, on the right.

Thus skew maps can generate chaotic attractors which are similar to two dimensional attractors.

While the presence of chaotic attractors in skew maps has been studied, results regarding the existence of more specific chaotic behavior involving attractors, such as crises and explosions, have not been published. The remainder of this paper will provide examples of their existence in skew maps. The similarities in the behavior of explosions and crises between skew maps and two-dimensional diffeomorphisms are

also discussed.

2.7 Crises

A crisis is a discontinuous change in the size of a chaotic attractor as a parameter is varied [3]. Their existence has been proven in one-dimensional maps and two-dimensional diffeomorphisms; for example, in two dimensions, the Hénon map produces a two-piece attractor which merges at a critical value to form a one-piece attractor [4]. The merging of the two pieces of the attractor coincides with the collision of the two pieces with a saddle fixed point located between them. Similar dynamics occur in our examples.

Using two maps that are known to generate crises, the logistic map and the Hénon map [4], a skew map system can be designed:

$$f(x) = \lambda x(1-x), \quad g(x,y) = a + dy - x^2 \tag{2.7}$$

Setting the parameters a to 1.4, d to 0.3, and allowing λ to vary, a two-piece attractor forms for λ just past 3.5. There is a fixed point located between the two pieces of the attractor, which can be calculated analytically as $X_0 = (\frac{\lambda-1}{\lambda}, 2-(\frac{\lambda-1}{\lambda})^2)$. The stable manifold of X_0 consists of vertical lines at the fixed point and its preimages, namely $x = \frac{\lambda-1}{\lambda}$ (at the fixed point), $x = \frac{1}{\lambda}$ (the first preimage), $x = \frac{\lambda \pm \sqrt{\lambda^2-4}}{2\lambda}$ (the second set of preimages), etc.

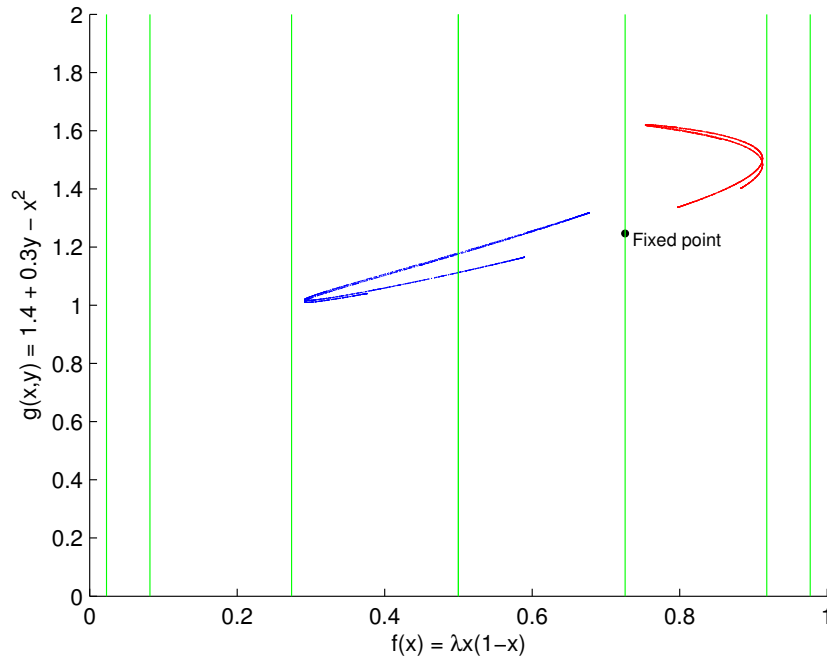At $\lambda = 3.65$, the attractor shows up as two very distinct pieces (see Figure 2.9).

Figure 2.9: The second iterate crisis map at $\lambda = 3.65$.

The fixed point X_0 is located in between the two pieces of the attractor, shown here in red and blue. The stable manifold is shown in green.

Each piece of the attractor is a branch of the unstable manifold of the fixed point X_0. If the dynamical system is redefined as the second iterate of the system defined by equation (2.7), then the attractor produced for a given initial value (x,y) of the system would be either one branch of the unstable manifold or the other: for $x < \frac{\lambda-1}{\lambda}$, the attractor is the branch on the left; for $x > \frac{\lambda-1}{\lambda}$, the attractor is the right branch.

The new equations for the system are:

$$f(x) = \lambda^2 x(1-x)(1 - \lambda x + \lambda x^2), \quad g(x,y) = a + d(a + dy - x^2) - \lambda^2 x^2 (1-x)^2 \quad (2.8)$$

Increasing the value of λ just slightly shows each piece of the attractor expanding

and approaching a tangency with three pieces of the stable manifold (see figure 2.10).
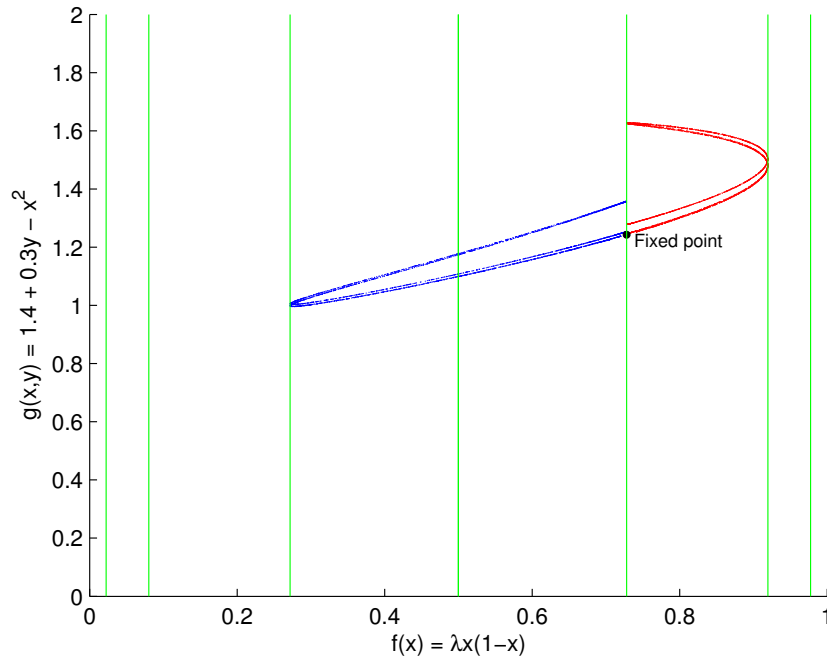

Figure 2.10: The second iterate crisis map at $\lambda = 3.678$.

Each piece of the attractor is approaching a tangency with two pieces of the stable manifold, as well as approaching the fixed point X_0.

As λ is increased further, it is difficult to determine whether the two pieces of the attractor are on different sides of the $x = \frac{\lambda-1}{\lambda}$ line. However, magnifying the area of the graph around the fixed point, it is clear from the isolation of the two colors on either side of the $x = x_0$ line that the two pieces are still distinct (see Figure 2.11).
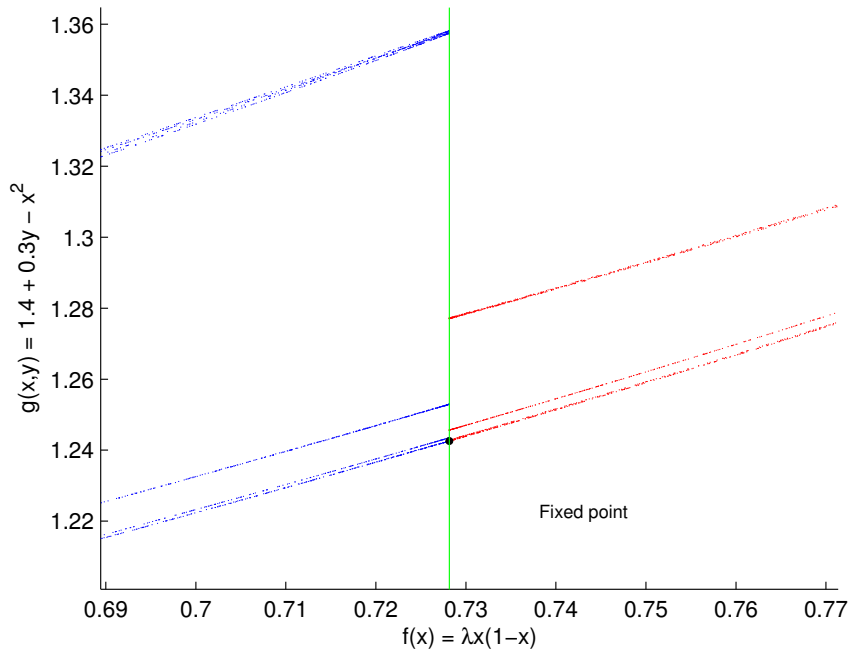
Figure 2.11: The second iterate crisis map at $\lambda = 3.6785735$.

A magnified view of the attractor close to the fixed point.

However, just past $\lambda = 3.6785735$, the two pieces of the attractor merge. Thus, for the system defined by (2.9), each piece of the attractor increases discontinuously in size at the critical point and incorporates the other piece of the attractor into itself.

This is shown by Figure 2.12, in which the iterates of each piece of the attractor now appear on both sides of the $x = \frac{\lambda-1}{\lambda}$ stable manifold.
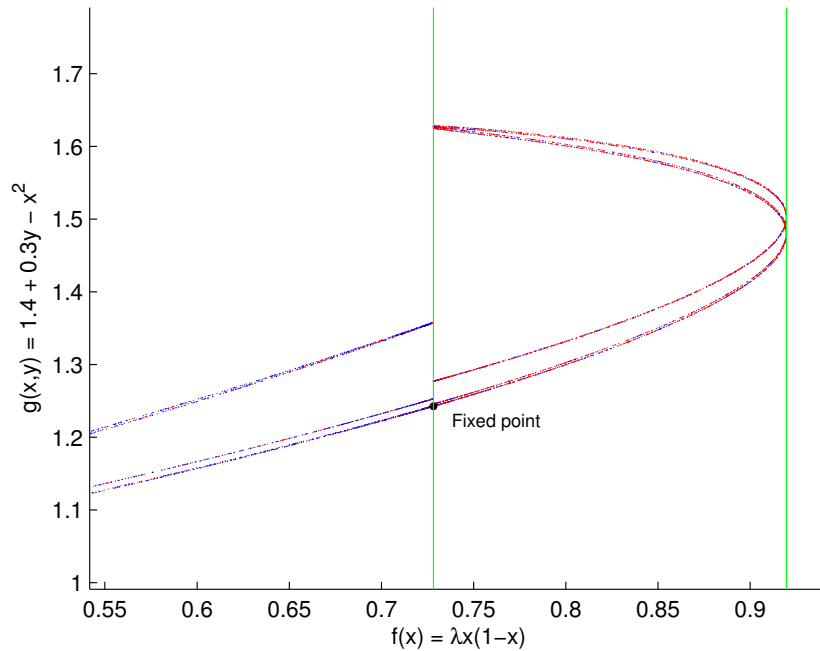
Figure 2.12: The second iterate crisis map at $\lambda = 3.6785736$.

A slightly magnified view of the attractor close to the fixed point, after the crisis value. Red and blue points, signifying each piece of the attractor, are shown on both sides of the stable manifold and along the length of each piece of the attractor.

At the critical value of λ, both pieces of the attractor are tangent at multiple places to the three pieces of the stable manifold. The lowest branch of each of the two pieces of the attractor also meet at the fixed point. Once λ increases past the critical value, both pieces of the attractor cross the stable manifold, which corresponds to the merging of the two pieces of the attractor.

This behavior is clearer at a slightly larger value of λ (see Figure 2.13).
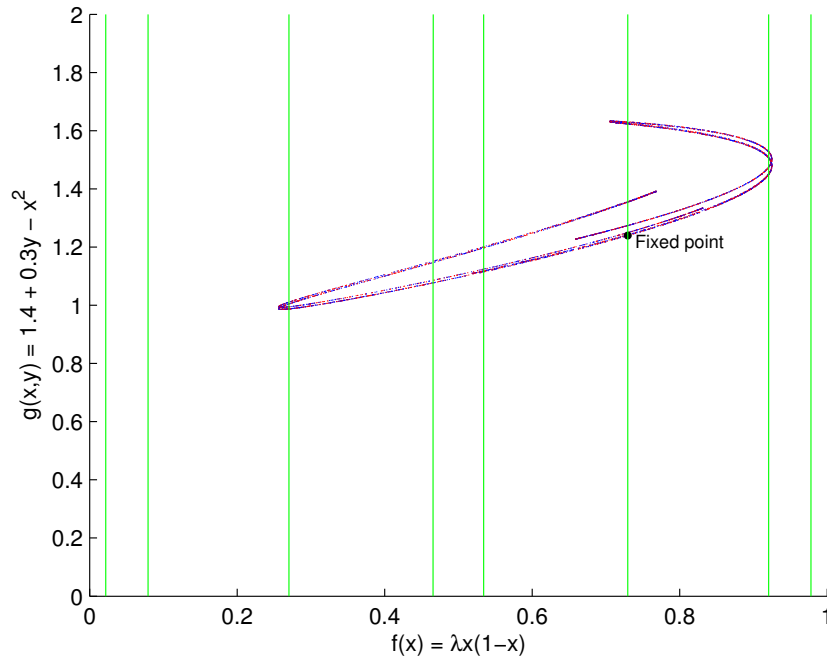
Figure 2.13: The second iterate crisis map at $\lambda = 3.7$.

The one-piece attractor, signified by red and blue iterates along the entire length. Each branch of the attractor crosses the piece of the stable manifold to which it was tangent at the critical value.

To summarize, the behavior of the map defined by equation (2.7) is very similar to the original Hénon map. The behavior at the crisis value is the same, where the two pieces of the attractor generated by the second iterates of the map merge together. The shape of the attractor is also similar; the primary difference is the shape of the stable manifold of the fixed point X_0. For the skew map, the stable manifold is composed of vertical lines; for the two-dimensional map, the stable manifold is a set of curves. The difference is due to the structure of skew maps, which forces the stable manifold in the $\begin{pmatrix} 0 \\ 1 \end{pmatrix}$ direction.

In the next section, a similar map will be used to illustrate the existence of explosions in skew maps.

2.8 Explosions

Explosions have been studied for one-dimensional maps and two-dimensional diffeomorphisms but not for skew maps. To determine when we might have an explosion in a skew map, we begin by analyzing the one-dimensional case. For one-dimensional maps, explosions can be generated via homoclinic tangencies, which are tangencies of the graph of the map at a homoclinic point. From the discussion in [13], we can come up with a series of assumptions that will lead to an explosion point:

1. $x \mapsto f_\lambda(x) : R \to R$ is a C^1 smooth family of C^2 interval maps.

2. For $\lambda = \lambda_0$, the critical value, there are no intervals on which f_{λ_0} is constant.

3. For f_{λ_0}, there is at most one of the following: (i) A non-hyperbolic fixed point or periodic orbit, or (ii) One critical point which comprises a tangency between stable and unstable manifolds of fixed points or periodic orbits.

4. For each λ, x_λ is a repelling fixed point for f_λ, and for f_{λ_0}, y is homoclinic to x_{λ_0}.

5. At $\lambda = \lambda_0$, the homoclinic orbit containing y contains only one critical point.

6. At f_{λ_0}, a point y is a homoclinic tangency point of x_{λ_0} contained in (at least one) homoclinic orbit $(z_{-k})_{k=0}^\infty$. Let L be such that $y = z_{-L}$.

If $f'(x_{\lambda_0}) > 0$, the left and right branches of the unstable manifold of x_{λ_0}, U_{Left} and U_{Right} respectively, are locally disjoint. We can now define a crossing orbit:

Assume the above six conditions hold. Then for g $:= f_{\lambda_0}^{L-1}$, z_{-1} is a point of

tangency. If for sufficiently large k, either (i) $z_{-k} \in U_{left}$, and the graph of g is locally above the horizontal line at z_{-1}, or (ii) $z_{-k} \in U_{right}$, and the graph of g is locally below the horizontal line at z_{-1}, then the homoclinic orbit (z_{-k}) is a crossing orbit.

Adding an additional condition:

7. At λ_0, the tangency point y is contained exclusively in one manifold branch of x_{λ_0}.

leads to our desired result:

Theorem 2.1. Assume the above seven conditions. If every homoclinic orbit containing y is a crossing orbit, then (y, λ_0) is an explosion point.

To summarize, given certain conditions about the map $x \mapsto f(x)$ where $f : R \to R$, a homoclinic tangency point y is an explosion point if it is contained in one branch of the unstable manifold of a fixed point x_0, but not in the other branch of the unstable manifold of x_0. The preimages of the explosion point will also be explosion points [3]. Figure 2.14 illustrates this situation.

For two-dimensional diffeomorphisms, a similar requirement holds for heteroclinic tangencies that certain branches of the stable and unstable manifolds must lie across the tangency from each other [1]. Therefore, it is very likely that explosions in skew maps are governed by similarly restrictive conditions. Therefore, the results for one-dimensional maps will be used to create a skew map example.

The basic shape of the graph depicted in Figure 2.14 can be replicated by

$$f(x) = \lambda x(1 + x)(1 - x)^2 \tag{2.9}$$

The resulting graph, however, is closer to a mirror image of Figure 2.14 reflected across the x = 0 axis. However, equation (2.9) does display chaotic behavior similar
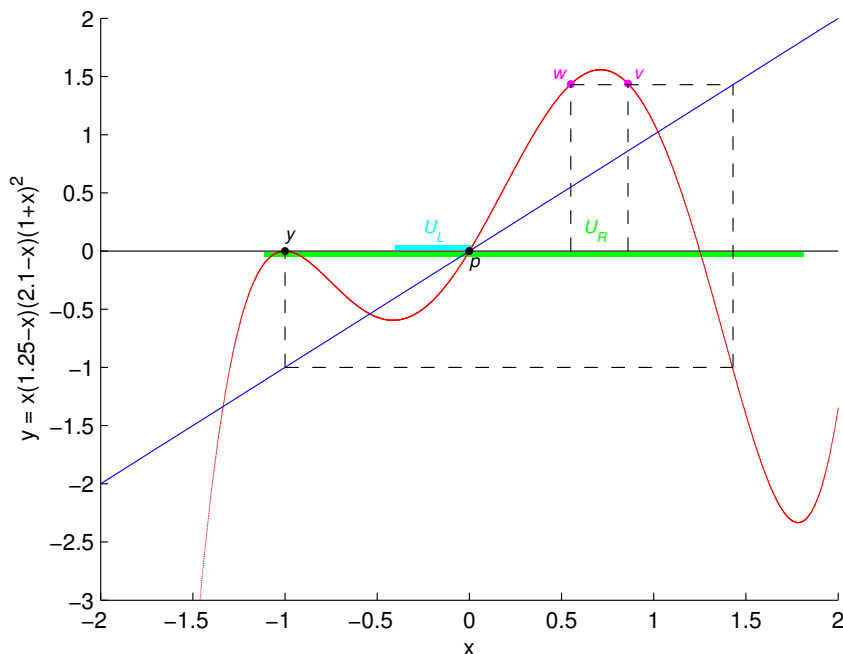
Figure 2.14: Explosion point for a homoclinic tangency.

y is a homoclinic tangency point which is contained in U_R but not U_L, where U_R and U_L are the iterates of the left and right branches of the unstable manifold of the fixed point p. It is therefore an explosion point. The preimages of y, w and v, are also explosion points [3].

to the logistic map for $0 < \lambda < 6.272$, with period doubling, the existence of chaotic attractors, and the formation of a crisis between a period three orbit and a chaotic attractor.

Since g(x,y) from our last example, $g(x, y) = a + dy - x^2$, assisted in producing an example of a crisis in a skew map, we shall use the g(x,y) from equation (2.7) and set f(x) as in equation (2.9). The new system then becomes:

$$f(x) = \lambda x(1 - x)^2(1 + x), \quad g(x, y) = 1.4 + 0.3y - x^2$$

which is equation (2.6).

As shown by Figures 2.4, 2.5, and 2.6 in the section on period doubling cascades, the map given by equation (2.6) exhibits period doubling for $\lambda > 1.24$, and a chaotic attractor appears for $\lambda > 1.43$ (see Figure 2.15).
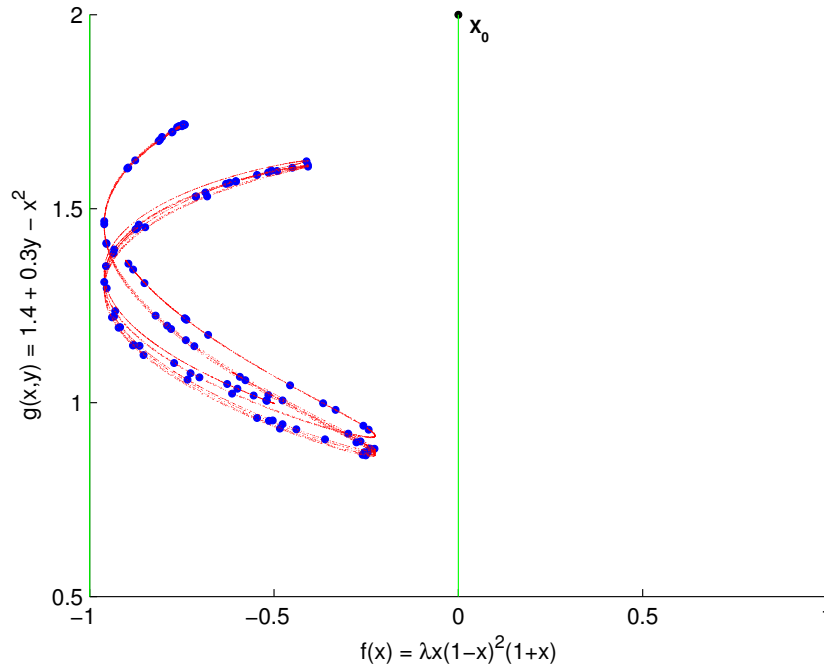

Figure 2.15: The attractor for the explosion map at $\lambda = 1.55$.

100 random points in the basin of attraction were iterated, with the first 500 iterates dropped, and the remaining 1,000 plotted in red. The blue dots signify the $1,500^{th}$ iterate of each random point. The green lines represent the pieces of the stable manifold of the fixed point X_0 located near the attractor.

As the value of λ increases, the attractor grows in size, and begins to approach the pieces of the stable manifold of the fixed point $X_0 = (0,2)$ (see Figure 2.16).
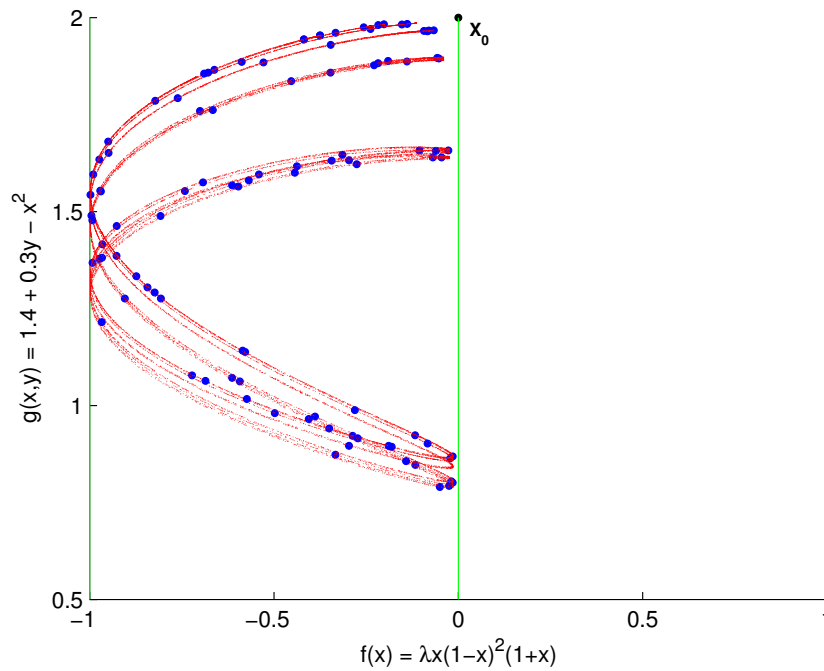

Figure 2.16: The attractor for the explosion map at $\lambda = 1.61$

The attractor approaches the stable manifold lines $x = -1$ and $x = 0$. The blue dots signify that the $1,500^{th}$ iterate of each initial point is still on the attractor.

As λ approaches the critical value $\lambda_0 \approx 1.6137247$, the attractor approaches a tangency with the stable manifold lines x = -1 and x = 0. The uppermost branch of the attractor also approaches an intersection with the fixed point X_0.

After $\lambda = \lambda_0$, the chaotic attractor no longer exists. The orbits of points in the basin of attraction (other than fixed or periodic points) will approach the region that was the chaotic attractor and spend many iterations around it, but will eventually leave the area, cross over the stable manifold at the fixed point X_0, and converge to the fixed point between x = 0 and x = 1 (see Figure 2.17).
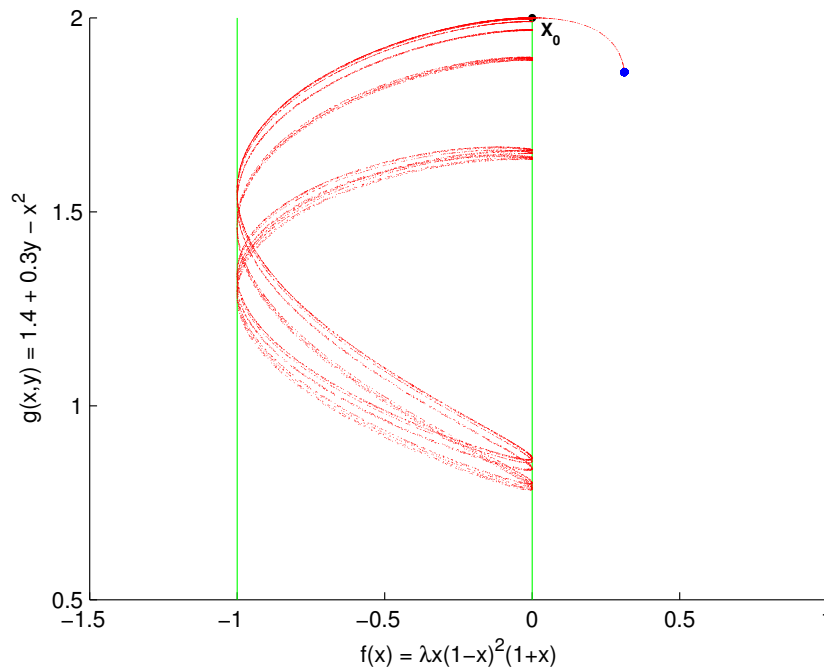

Figure 2.17: The attractor for the explosion map at $\lambda = 1.61373$.

Orbits around the chaotic attractor eventually leave and cross the stable manifold at X_0. The blue dot shows that the $1,500^{th}$ iterate of each of the 100 initial points has left the region of the attractor and converged to the fixed point in the $x \in (0,1]$ range.

The merging of the attractor with the fixed point, and the orbit that crosses the x = 0 axis at the fixed point, are more easily shown by a magnified view close to the fixed point X_0 for λ greater than but very close to λ_0 (see Figure 2.18).
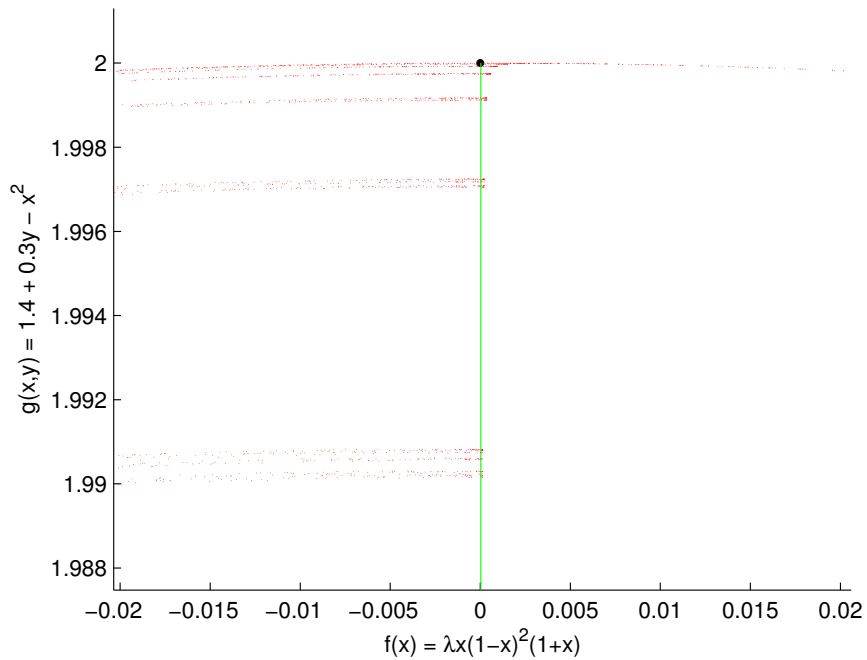

Figure 2.18: A magnification of the attractor for the explosion map at $\lambda = 1.61373$.

A magnification of the attractor at $\lambda = 1.61373$ close to the saddle fixed point X_0. Each branch of the attractor has crossed the stable manifold at $x = 0$, and the orbit crosses completely over to the $x \in (0, 1]$ region at the fixed point.

As λ is steadily increased past λ_0, the iterates converge more quickly to the new fixed point and spend less time in the vicinity of the former attractor. This behavior is called transient chaos [4].

Figures 2.19 and 2.20 demonstrate this point. At λ extremely close to but greater than λ_0, the iterates spend a considerable amount of time around the region of the former attractor, as indicated by the density of the attractor shown in Figure 2.19.
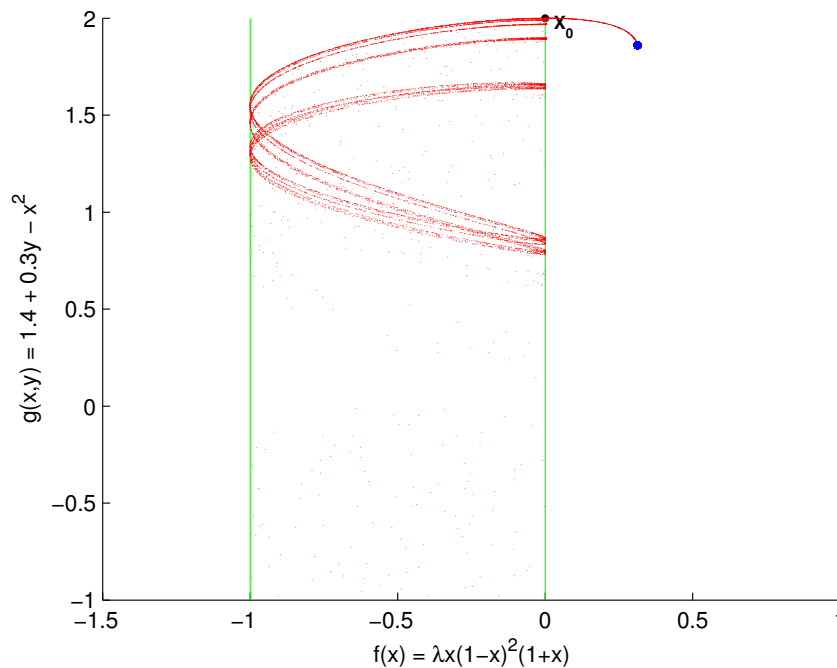

Figure 2.19: All iterates of the explosion map at $\lambda = 1.614$.

100 points were randomly selected in the basin of attraction of the former attractor, and 1,000 iterates were plotted (no iterates were dropped, including the original values). The blue dot is the value of the $1,000^{th}$ iterate of all random points. The density of the points in the region of the former attractor signify the iterates still spent considerable time around the former attractor before converging to the fixed point.

However, as λ is increased further past λ_0, the iterates spend less time around the former attractor and converge more quickly to the attracting fixed point in the region $(0,1]$, as shown in Figure 2.20.
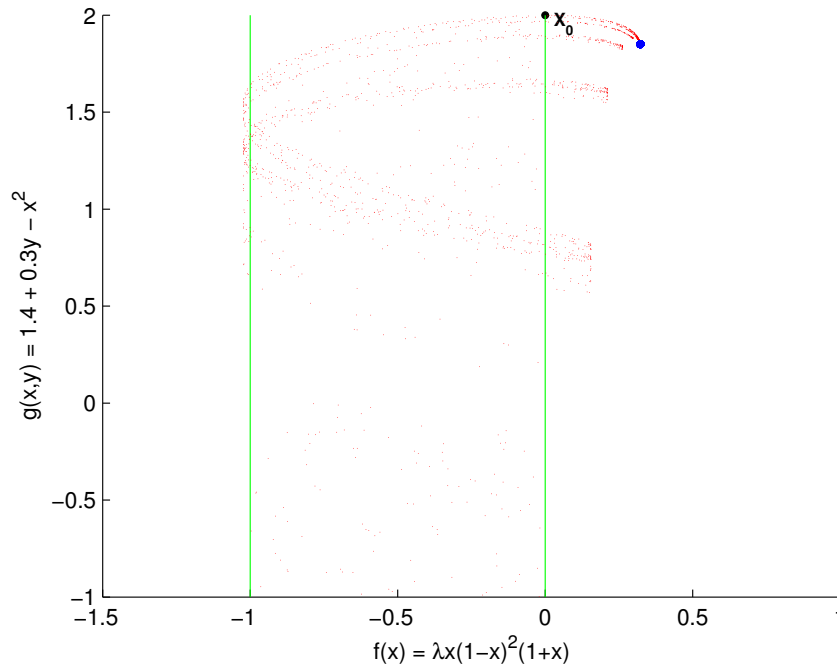

Figure 2.20: All iterates of the explosion map at $\lambda = 1.65$.

The density of the points in the region of the former attractor has decreased significantly from the previous graph.

To summarize the results, prior to the critical value λ_0, any point in the basin of attraction with $x \in [-1, 0)$ will converge to the chaotic attractor. A point $x \in$ the attractor will stay on the attractor, and thus $x \in \omega(x)$. Thus x is a chain recurrent point.

After λ_0, any point in the basin of attraction of the former attractor will converge to the fixed point in $(0,1]$ rather than to the chaotic attractor, so $x \notin \omega(x)$ for all $x \in [-1, 0)$. So x is no longer chain recurrent. Thus, we have an explosion at the parameter value $\lambda_0 \approx 1.6137247$ and the fixed point $(0,2)$ due to the change in the size of the chain recurrent set for points along the attractor.

The results of this example follow closely with the dynamics of an orbit of the Ikeda map $f_r(z) = r + 0.9ze^{i(0.4 - \frac{6.0}{1+|x|^2})}$ [4, page 420], which exhibits transient chaos at r = 1.003. For both maps, once the bifurcation value has been exceeded, the ω-limit set of the basin of attraction changes from a chaotic attractor to a fixed point. The iterates travel close to the area of the former attractor for a period of time before converging to the fixed point, and the further the parameter value is from the critical value, the less time the iterates take to converge to the fixed point.

A final point: the dynamics of the map given by equation (2.6) at the critical value λ_0 may be more complicated than has been shown. Using the Dynamics software, other saddle points (other than the fixed point at X_0) can be found extremely close to the attractor at λ_0:

- A saddle fixed point located toward the lower edge of the attractor;
- A period two saddle that is located in the middle of the attractor;
- Two period three saddles located inside the attractor; and
- Three period four saddles located inside the attractor.

Given this information, we expect that there are infinitely many periodic orbits close to the attractor.

Chapter 3: Conclusion

3.1 Results

Smooth skew maps exhibit chaotic behavior similar to that for one-dimensional maps and two-dimensional diffeomorphisms. However, certain behaviors are limited to the dynamics in one dimension. Homoclinic orbits for skew maps must have a snap-back repeller in the x-direction, and unstable manifolds may cross one another, which is possible in one-dimensional maps but not for two-dimensional diffeomorphisms.

However, other aspects of chaotic dynamics are present in all three types of maps. Adherence to Feigenbaum's law for period doubling cascades is consistent for all three maps, as is the existence and behavior of chaotic attractors.

The purpose of this thesis was to study crises and explosions and determine whether they are present in skew maps. From the results given in this paper, we have illustrated their existence in skew maps and have highlighted the similarities in behavior to well known two-dimensional diffeomorphisms (the Hénon map and the Ikeda map respectively).

However, for both sets of skew map examples that showed the existence of crises and explosions, there was one-dimensional structure present in the f(x) function. The logistic map f(x) = λx(1-x) used for the crisis example undergoes several crises itself as λ varies between 3 and 4. Similarly, the quartic map given by equation (2.9) used for the explosion example was modeled on a map known to produce explosion points.

So although the results mimic those for the Hénon map and the Ikeda map, the existence of crises and explosions in skew maps may depend more on their existence in the one-dimensional case than on two-dimensional diffeomorphisms.

3.2   Areas for Further Study

Thus, an area for further study would be to remove the chaotic behavior present in f(x) and look for dynamics in the g(x,y) function that would produce a crisis or explosion point. In doing so, some of the chaotic dynamics could be kept in f(x), but not the particular behavior we are trying to prove (for example, an f(x) that produced a crisis but not an explosion could be tried in an effort to show whether an explosion exists in a slightly more generic skew map.)

Since a fair amount is known about crises and explosions for one-dimensional maps and two-dimensional diffeomorphisms, it is logical to use those assumptions to understand how explosions are produced in skew maps. But another alternative would be to find behavior that is unique only to skew maps, or to analytically rule out the possibility that there is chaotic behavior unique to skew maps.

Bibliography

Bibliography

[1] K. Alligood, E. Sander, and J. Yorke. Explosions: Global bifurcations at heteroclinic tangencies. *Ergodic Theory and Dynamical Systems*, 22:953–972, 2002.

[2] K. Alligood, E. Sander, and J. Yorke. Crossing bifurcations and unstable dimension variability. *Physical Review Letters*, 96:244103 1–4, 2006.

[3] K. Alligood, E. Sander, and J. Yorke. Explosions in dimensions one through three. *Rendiconti del Seminario Matematico, Torino*, 65(1), 2007.

[4] K. Alligood, T. Sauer, and J. Yorke. *Chaos - An Introduction to Dynamical Systems*. Springer-Verlag, New York, NY, 1996.

[5] F. Balibrea and J. Smítal. A triangular map with homoclinic orbits and no infinite ω-limit set containing periodic points. *Topology and its Applications*, 153:2092–2095, 2006.

[6] G-L. Forti, L. Paganoni, and J. Smítal. Triangular maps with all periods and no infinite ω-limit set containing periodic points. *Topology and its Applications*, 153:818–832, 2005.

[7] J. Hale and H. Koçak. *Dynamics and Bifurcations*. Springer-Verlag, New York, NY, 1991.

[8] K. Josić and E. Sander. The structure of synchronization sets for noninvertible systems. *Chaos*, 14:249–262, 2004.

[9] J. Kupka. The triangular maps with closed sets of periodic points. *Journal of Mathematical Analysis and Applications*, 319:302–314, 2006.

[10] F. Marotto. Snap-back repellers imply chaos in r^n. *Journal of Mathematical Analysis and Applications*, 63:199–223, 1978.

[11] C. Robinson. *Dynamical Systems - Stability, Symbolic Dynamics, and Chaos*. CRC Press, Boca Raton, FL, 1999.

[12] A. Kuznetsov S. Kuznetsov and I. Sataev. Multiparameter critical situations, universality and scaling in two-dimensional period-doubling maps. *Journal of Statistical Physics*, 121(5/6), December 2005.

[13] E. Sander and J. Yorke. A classification of explosions in dimension one. *Preprint*, 2007.

Curriculum Vitae

The author received her Bachelor of Science in Mathematics and Bachelor of Arts in Liberal Arts and Sciences from Virginia Polytechnic and State University in 1988.

She began a career in finance in 1994, which led to increasingly responsible positions in both the public and private sectors. However, her interest in pure mathematics and the need for intellectual stimulation never faded, and in 2004 she decided to return to graduate school to pursue a Masters degree in Mathematics.

After the completion of this thesis and her Masters degree at George Mason University, she will continue her studies towards a PhD.